

Spin-polarized two-dimensional electron/hole gases on LiCoO₂ layers.

Santosh Kumar Radha and Walter R. L. Lambrecht
Department of Physics, Case Western Reserve University,
10900 Euclid Avenue, Cleveland, OH-44106-7079

First-principles calculations show the formation of a 2D spin polarized electron (hole) gas on the Li (CoO₂) terminated surfaces of finite slabs down to a monolayer of LiCoO₂ in remarkable contrast with the bulk band structure stabilized by Li donating its electron to the CoO₂ layer forming a Co- $d - t_{2g}^6$ insulator. By mapping the first-principles computational results to a minimal tight-binding models corresponding to a non-chiral 3D generalization of the quadripartite Su-Schrieffer-Heeger (SSH4) model, we show that these surface states have topological origin.

LiCoO₂ has been mostly studied as cathode material in Li-ion batteries.[1–3] However, its layered structure also lends itself to the possibility of extracting interesting ultrathin mono- or few layers nanoflakes. A chemical exfoliation procedure has recently been established by Pachuta *et al.* [4] and similar exfoliation studies have also been done on Na_xCoO₂. [5] The $R\bar{3}m$ structure of LiCoO₂ consists of alternating CoO₂ layers, which consist of edge sharing CoO₆ octahedra, and Li layers stacked in an ABC stacking. By replacing lithium by large organic ions, the distance between the layers swells and they can then be exfoliated in solution and redeposited on a substrate of choice by precipitation with different salts.

Inspired by these exfoliation experiments we investigated the electronic structure of LiCoO₂ few layer systems with various Li and other ion terminations and as function of thickness of the layers using density functional theory (DFT) calculations.[6, 7] In the process, we found, surprisingly that Li no longer fully donates its electron to the CoO₂ layer but instead a surface state appears above the Li and is occupied with a fraction of an electron (~ 0.25) per Li. The amount of charge residing in this surface state was found to be remarkably robust as function of thickness of the number of LiCoO₂ layers, indicating that this is a surface rather than ultrathin film effect.

As we will show, the Li bands in bulk LiCoO₂ lie at energies $E > 5$ eV above the Fermi level, consistent with the mostly ionic charge donation picture mentioned above. So, the fact that a Li related surface state comes down sufficiently close to the Fermi level to become partially occupied is truly surprising. Furthermore because it is accompanied by the opposite surface CoO₂ becoming spin-polarized it leads actually to a spin-polarized electron gas on the Li side which is located primarily above the Li atoms. Apart from the possibilities this may offer for interesting physics, the main question we address in this paper is: why does this happen? The answer we propose is that this is a topological effect. We show that the DFT calculations can be explained by a minimal tight-binding (TB) model, closely related to the quadripartite Su-Schrieffer-Heeger (SSH4) model which has been shown to support topologically protected sur-

face states for specific conditions on the interatomic hopping integrals.[8] However, while the original SSH4 model has chiral symmetry protecting the surface state at zero energy, in the present case, the Li/CoO₂ electronegativity difference leads to surface states which would tend to still place the surface electrons on the CoO₂ side. The crucial element that allows the Li surface state to become partially filled is the strong lateral interaction between Li atoms on the surface. The resulting band broadening leads the Li surface band to dip below the top of the CoO₂ localized surface band leading to a partial electron/hole occupation in these bands respectively. As a further proof of the importance of the lateral interaction, we find that when we place 1/2 Li per cell on opposite sides of the slab, whereby the Li occur along 1D rows, the Li surface band has then only 1/3 of the band width and no longer dips below the Fermi level.

We start by comparing the band structure in bulk LiCoO₂ with that of a monolayer LiCoO₂ in Fig. 1 (a) and (b). In the bulk case, we find an insulating band structure with a gap between the filled t_{2g} and e_g bands Co- d . The Li s and p derived bands, highlighted in color occur at high energy indicating that they donate their electron to the Co- t_{2g} orbitals and support a mostly ionic picture of the bonding. In strong contrast, in the monolayer system, we find an additional set of spin-polarized bands, as highlighted in the figure by yellow shading. By orbital decomposition, it is clear that this band is Li related and its 2D dispersion closely matches that of a hypothetical 2D monolayer of Li atoms. Importantly, we also find that it has not only Li- s but also Li- p_z character indicating the formation of Li- sp_z hybrid states. This free-electron-like band has clearly avoided crossings with the Co- e_g bands around 2 eV. It dips down below the Fermi level with an electron pocket near Γ . Inspection of the corresponding wavefunction modulo squared shown in the inset below it shows clearly that it is a surface state hovering slightly above the Li atom. This band depends somewhat on the location chosen for the Li atom, as shown in Supplemental Material (SM),[9] but its general characteristics are robust. In the lowest energy structure it is found to be spin polarized as seen by the splitting of the up and down spin bands and indi-

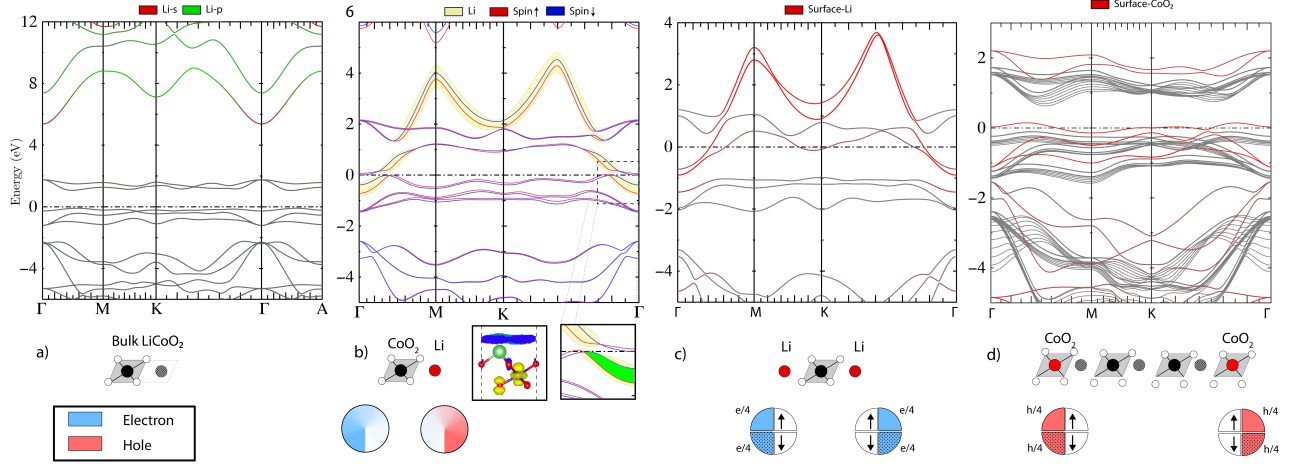


FIG. 1. (a) Bulk band structure of LiCoO_2 , (b) Spin polarized 2D LiCoO_2 mono-layer. The *green* region in the rightmost inset below (corresponding to the dashed line box in the band figure) shows the spin polarization in the 2DEG. The inset on its left shows the density of the wave function at Γ of the Li band in dark blue. (c) Li terminated LiCoO_2 with 2D electron gas (d) CoO_2 terminated LiCoO_2 with 2D hole gas. The circles colored red and blue below the figures indicate the fractionalization of the charge in the surface states. In panels (c,d) it is determined by symmetry whereas in (b) it depends on the band parameters. The structural model corresponding to each case is also indicated below the corresponding band figure.

cated by green shading in the inset below. The fact that its maximum density lies above the Li atom is consistent with a sp_z hybrid orbital derived band. A comparison of the bands for different Li locations in the surface unit cell is given in SM.[9] Further inspection of a planar average of the the total electron density of the LiCoO_2 and integrating this in the z region from just above the Li site into the vacuum indicates a total charge of $\sim 0.25 e$. This corresponds to a rather high density of $5 \times 10^{14} e/\text{cm}^2$. However we need to point out that this precise value depends on the cut-off of the spatial region over which we integrated. Further calculations for thicker slabs with 3 and 4 layers with the same termination of one Li terminated and one CoO_2 terminated surface indicate that the surface charge density is remarkably robust. Orbital decomposition in these thicker slabs shows that a second surface state occurs near the Fermi level and is localized on the opposite CoO_2 terminated surface layer and crosses the Li related one. We find that there is a net hole concentration on that layer.

To rule out that this would be a supercell artifact arising from the polar nature of the structure, in which an artificial dipole could arise over the vacuum region, we also consider a symmetrical slab with both surfaces Li terminated. In this case, the system is in some sense overcompensated by having one additional Li. The band structure for this case is shown in Fig. 1(c). A similar surface state is then found on both both Li terminated surfaces and, in fact, one can see that the occupied electron pocket in this band near Γ is larger. We will later show that for symmetry reasons it must contain a fractionalized $e/2$ for each spin, so a net charge of 1 electron per Li but for each spin it is in a single state

spread equally over both surfaces. Similarly, in the case of a symmetric CoO_2 termination a partially filled surface state occurs on both surface layers with equal hole concentration by symmetry. This is shown in Fig. 1(d).

We also considered a $1/2$ Li per Co symmetrically at both terminating surfaces. In that case the Li is placed in 1D rows on the surface and a 1D electron gas is found above these Li rows, as shown in SM.[9] However, the density of electrons in this case is smaller by about a factor 10. We further inspect the dilute limit of 1 Li per 4 Co atoms and still find an even smaller residual small charge density in an orbital locally above that Li. However, no Li localized surface state dipping below the Fermi level is found in these cases with a reduced Li surface concentration. This indicates that sufficient lateral interaction between Li atoms is required to generate a significant occupation of the surface states with electrons. Replacing the Li terminating layer by Be (also overcompensating the system from the CoO_2 point of view) we find a higher electron density in a Be related surface band. Replacing Li by Na gives similar results but with different band widths of the surface band because of the stronger overlap of the Na orbitals. The band structures of these cases are all shown in SM.[9].

To explain these remarkable results, we now consider a minimal tight-binding model. First, it is clear that the Li needs to be represented by two sp_z orbitals pointing toward the CoO_2 layer on either side. It is well known that an even number of orbitals is required in a 1D model to obtain topologically non-trivial band structures. Therefore we choose to represent the CoO_2 layer by two s -like Wannier orbitals. One could think of these as representing the a_1 -symmetry of the D_{3d} group or d_{z^2} or-

bitals on Co with z along the layer stacking \mathbf{c} -axis making bonding orbitals with $\text{O-}p_z$ on either side of the Co. Of course, this does not represent the full set of CoO_2 layer derived bands but we will argue that it represents the relevant bands leading to the surface states. The important point is that the CoO_2 and Li each are represented by two Wannier type orbitals whose centers are not on the atoms but on the bonds in between atoms in the layer stacking direction.

This minimal model is then a non-chiral version of the SSH4 model. Ordering the orbitals as $\{|Li^a\rangle, |CoO_2^a\rangle, |Li^b\rangle, |CoO_2^b\rangle\}$ the Hamiltonian for the above 1D system (with distance between the layers set to 1) is represented by the following 4×4 matrix:

$$H_{1d} = \begin{pmatrix} \delta & 0 & \tau_1 & \tau_4 e^{ik_z} \\ 0 & -\delta & \tau_2 & \tau_3 \\ \tau_1 & \tau_2 & \delta & 0 \\ \tau_4 e^{-ik_z} & \tau_3 & 0 & -\delta \end{pmatrix}, \quad (1)$$

$$= \begin{pmatrix} \delta \sigma_z & \mathbf{s}^*(k_z) \\ \mathbf{s}(k_z) & \delta \sigma_z \end{pmatrix} \quad (2)$$

$$= \sigma_x \otimes \mathbf{h}(k_z) - i\sigma_y \otimes \mathbf{a}(k_z) + \delta \mathbb{1}_2 \otimes \sigma_z \quad (3)$$

where τ_1, τ_2, τ_3 , are intra-unit cell interaction while $\tau_4 = \tau_2$ is the out of unit cell interaction, δ is the ionic on-site term for Li relative to CoO_2 . The second form of the Hamiltonian focuses on its 2×2 block structure, in which $\mathbf{s}(k_z)$ is a 2×2 matrix which is split in its hermitian, $\mathbf{h}(k_z) = \mathbf{h}(k_z)^\dagger$, and anti-hermitian, $\mathbf{a}(k_z)^\dagger = -\mathbf{a}(k_z)$, parts, allowing us to finally write the block structure of the Hamiltonian in terms of the Pauli matrices and a 2×2 unit matrix $\mathbb{1}_2 = \sigma_0$. For our system, $\tau_2 = \tau_4 = t_{\text{Li-CoO}_2}^z$ corresponds to the interaction between the Li and CoO_2 layers while $\tau_1 = t_{\text{Li}}^z = (E_s^{\text{Li}} - E_p^{\text{Li}})/2$ corresponds to the interaction between the two Li sp_z 's on the same Li atom, and $\tau_3 = t_{\text{CoO}_2}^z$ to O-Co-O interaction within the layer.

This model, which is the SSH4 model for $\delta = 0$ corresponding to chiral symmetry, has been shown [8] to have non-trivial topology which requires zero-energy edge states when $\tau_1 \tau_3 < \tau_2 \tau_4$. In fact, in that case, the winding number, which characterizes the topology $\mathcal{W} = \oint \frac{dk_z}{2\pi} \partial_{k_z} \arg \det\{s(k_z)\}$ is 1, while in the other case it is 0. This condition in our case, indicates that the covalent Li- sp_z - CoO_2 interaction is stronger than the intra CoO_2 interaction or the Li- sp_z interaction on the same Li atom.

When δ is not zero this model becomes non-chiral and the zero energy surface states move up and down in energy and become localized on opposite edges which would tend to localize the electrons on one side only, in the present case obviously the CoO_2 side because it would have lower energy $-\delta$ because of its electronegative character. Therefore, to explain the electron occupation of the Li-derived surface state, we need to generalize our model to include the lateral in-plane interactions.

We introduce in-plane t_{Li}^{xy} and $t_{\text{CoO}_2}^{xy}$ interactions on

the planar trigonal lattice

$$f_{Li(Co)} = 2t_{Li(Co)}^{xy} \sum_{i=1}^3 \cos(\mathbf{k} \cdot \boldsymbol{\delta}_i) \quad (4)$$

where $\pm \boldsymbol{\delta}_i$ are the 6 vectors pointing toward the nearest neighbors and $\mathbf{k}_{\parallel} = k_1 \mathbf{b}_1 + k_2 \mathbf{b}_2 = (k_x, k_y)$ is the in-plane 2D wave vector. This modifies only the diagonal terms in (2) leading to

$$H_{3d}(k_x, k_y, k_z) = \sigma_x \otimes \mathbf{h}(k_z) - i\sigma_y \otimes \mathbf{a}(k_z) + \sigma_0 \otimes [\delta + \Delta(\mathbf{k}_{\parallel})] \sigma_z \quad (5)$$

after we drop out a constant from the Hamiltonian diagonal. Here, $\Delta(\mathbf{k}_{\parallel}) = \frac{f_{\text{Li}} - f_{\text{Co}}}{2}$, is added to the δ in the 1D model and can be thought of as a dimensional crossover parameter,[10] which tunes the influence of the in-plane dimensions. Physically, $\Delta(\mathbf{k}_{\parallel})$ is proportional to the width of the energy bands in \mathbf{k}_{\parallel} space, which is $\Gamma = \Gamma_{\text{Li}} + \Gamma_{\text{CoO}_2} = 6(t_{\text{Li}}^{xy} + t_{\text{CoO}_2}^{xy})$.

Figure 2 (c) shows the 3D-layered tight-binding model and the corresponding hopping parameters described above. Figure 2 (d) shows the band structure of the above 3D Hamiltonian while (e) shows the energy levels of the 2D periodic system with a finite number of layers along the z -axis with top most layer having Li and bottom layer CoO_2 . The bands are color-weighted (Li-red, Co-blue). While the 3D periodic TB system is seen to have a wide gap between high-lying Li derived bands and low lying CoO_2 -derived bands, two surface bands with significant \mathbf{k}_{\parallel} dispersion are seen in part(e), which are respectively localized on the Li (red) and CoO_2 sides (blue) and are found to cross each other near the Fermi energy. In fact, we can see that besides the surface bands lying in the overall 3D gap, two more states have significant weight on the end Li and CoO_2 orbitals but they lie within the range of the bulk bands occurring in a gap in the projected bands but not in the overall gap between occupied and empty states.

The interlayer parameters used in the TB Hamiltonian are chosen to satisfy the SSH4 non-triviality criterion. The in plane interactions determining $\Delta(\mathbf{k}_{\parallel})$ are chosen to resemble the DFT band structure (shown in part (f) for a 14 nm thick (in the z -direction) in-plane periodic layer) and turn out to satisfy $t_{\text{CoO}_2}^{xy} \approx -0.1 t_{\text{Li}}^{xy}$. The opposite dispersion of these surface bands is obvious from the DFT results and translates to these in-plane directions having opposite sign. In the actual system, it is clear that $t_{\text{Li}}^{xy} < 0$ as it is a π -interaction between Li- p_z states combined with σ -interaction between the s -part of the sp_z orbitals and in absolute value is much larger than the $t_{\text{CoO}_2}^{xy} > 0$. This is important because it means that the Fermi level is pinned at the intersection of the two surface bands, which indicate an overall semimetallic case with as many holes in the CoO_2 surface band as there are electrons in the Li surface band when they overlap.

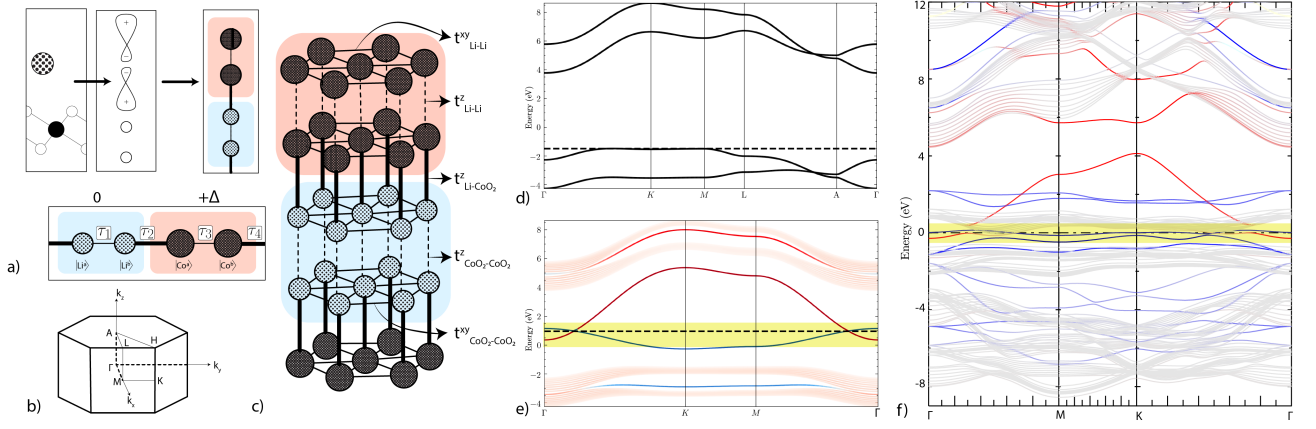


FIG. 2. a) LiCoO₂ unit cell along with orbitals after hybridization and the final model having all relevant physics b) 3D Hamiltonian considered for calculation and the BZ c) 3D model of the Hamiltonian and the corresponding hopping terms d) Bulk band of the 3D Hamiltonian. e) Band structure of a finite slab extending in $x-y$ direction. *red* color corresponds to the edge Li atom while *blue* to bottom most CoO₂ f) Spin-less DFT band structure of 14nm unit cell with Li terminated on one side and CoO₂ layer on another with colors representing the same as in previous figure.

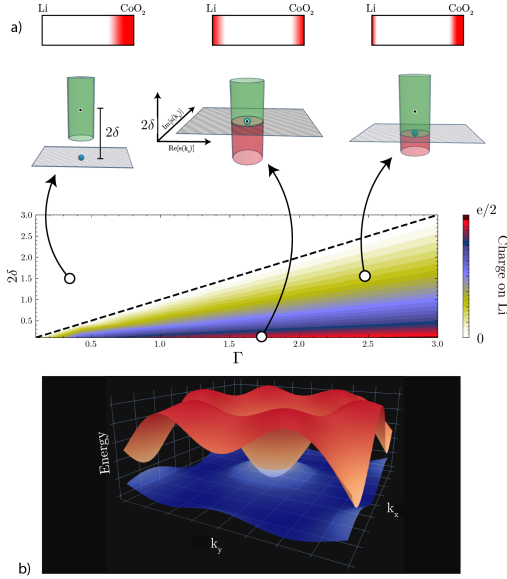


FIG. 3. (a) Schematic representation of Li and CoO₂ surface charge for different choices of model parameters, shown below in (b) cylinder topological model, (c) surface charge density on Li side (as color map) per Li calculated within the full TB model as function of on-site term δ and in-plane band width Γ , (d) 3D view of intersecting surface bands.

While we recognize that this model is representing only part of the bands of the actual physical system, the correspondence of the surface bands in the DFT and the TB-model Hamiltonian is convincing that it captures the essence of the relevant physics. Essentially, we thus conclude that the surface states originate from the topologically nontrivial SSH4 character of the interlayer bonds which correspond to a non-zero winding number. To this

is added a term in the Hamiltonian orthogonal to the space of the σ_x, σ_y parts of the Hamiltonian which define a complex plane in which the winding number is defined. One can generally write such a Hamiltonian as $H = \mathbf{d} \cdot \boldsymbol{\sigma}$ where d_{\parallel} corresponds to the (x, y) components in a complex plane defining the winding number.[11, 12] The loop defining the winding number is now above or below the complex plane. Its projection on the complex plane encircling the origin or not defines the winding number and therefore topological non-trivial/trivial character. The component d_{\perp} to this plane determines the energy position of the surface states $E_s = \pm |d_{\perp}|$, [12] away from zero by the chiral symmetry breaking. In the bipartite SSH model, the third component of the $\boldsymbol{\sigma}$ would be simply the third Pauli matrix σ_z while in our case it is $\sigma_0 \otimes \sigma_z$. However, because of the in-plane band dispersion, such an SSH4 like model now applies at each \mathbf{k}_{\parallel} . This turns the loop outside the plane into a cylinder (shown in Fig. 3(b) centered at energy 2δ from the plane with height given by the 2D band width).

The amount of charge on the Li is determined (shown in Fig. Figure 3(a,c) as function of the model parameters) by how much the bottom of the Li band overlaps with the top of the CoO₂ band, as shown in Fig. Figure 3(d). Assuming a steplike density of states (DOS) for each band near these band edges and parabolic free electron like bands, which makes sense near the band edges for a 2D system, we can easily determine the Fermi energy, located in the surface bands from the fact that the number of electrons in the upper band equals the number of holes in the lower band. Using the density of states for free electrons in 2D to be proportional to the effective mass in each band, and the proportionality of the inverse effective mass to the hopping parameter or bandwidth of

the tight-binding model for that band, we find that

$$\frac{\text{charge on Li-side}}{\text{charge on CoO}_2\text{-side}} = \begin{cases} \frac{\Gamma-2\delta}{\Gamma+2\delta}, & 2\delta \leq \Gamma \\ 0 & 2\delta \geq \Gamma \end{cases} \quad (6)$$

One can easily see that if the splitting of the two surface band centers (which is 2δ) is larger than the sum of half their band widths then the charge will still all be localized on the CoO_2 and zero on Li. A full numerical calculation of the net surface charge density within the tight-binding model resulting from the overlapping bands is given in SM and shown to closely agree with the above approximate result.[9] In the cylinder topological model mentioned above, the part of the cylinder that dips below the surface corresponding to $\delta = 0$ gives the amount of charge on the Li side, again when assuming a constant DOS.

The above model is consistent with the facts from our DFT calculations presented in the SM, that for Na with larger in-plane interactions and hence larger 2D surface band width, a larger surface charge density is found than for Li on the surface. The same is true for Be which also has a smaller electronegativity difference and hence smaller δ in our model and, in fact gives an additional electron to the surface states. Finally, when two equal surface terminations are used then there is an overall inversion/mirror symmetry in the center of the slab and thus by symmetry requires that the additional electron in the surface states is spread equally over both sides. The same is true for holes for the case of two CoO_2 terminated surfaces.

In the SM, we show furthermore that the occurrence of the surface states is related to the entanglement of the states in the two halves of the system that are separated by creating the surface by calculating the entanglement spectrum.[13–16]

In summary, we have shown that surfaces of LiCoO_2 finite slabs host topologically required surface states related to the SSH4 like nontrivial interlayer interactions of $\text{Li-}sp_z$ and CoO_2 bond-centered Wannier orbitals. As a result of strong lateral interactions, the Li related surface band can become partially occupied and host a spin-polarized 2DEG of fairly high electron density. While several angular resolved electron spectroscopy (ARPES) and scanning tunneling microscopy studies (STM) have been published in the past [3, 17–21] for both Li_xCoO_2 and Na_xCoO_2 they were generally focused on the bulk rather than on the search for surface states, which may thus have been missed.

Acknowledgements: This work was supported by the U.S. Air Force Office of Scientific Research under Grant No. FA9550-18-1-0030. The calculations made use of the High Performance Computing Resource in the Core Facility for Advanced Research Computing at Case Western Reserve University.

-
- [1] K. Mizushima, P. Jones, P. Wiseman, and J. Goodenough, *Materials Research Bulletin* **15**, 783 (1980).
 - [2] K. Miyoshi, K. Manami, R. Sasai, S. Nishigori, and J. Takeuchi, *Phys. Rev. B* **98**, 195106 (2018).
 - [3] K. Iwaya, T. Ogawa, T. Minato, K. Miyoshi, J. Takeuchi, A. Kuwabara, H. Moriwake, Y. Kim, and T. Hitosugi, *Phys. Rev. Lett.* **111**, 126104 (2013).
 - [4] K. G. Pachuta, E. B. Pentzer, and A. Sehirlioglu, *Journal of the American Ceramic Society* **0** (2019), 10.1111/jace.16382.
 - [5] Y. Masuda, Y. Hamada, W. S. Seo, and K. Koumoto, *Journal of Nanoscience and Nanotechnology* **6**, 1632 (2006).
 - [6] D. Pashov, S. Acharya, W. R. Lambrecht, J. Jackson, K. D. Belashchenko, A. Chantis, F. Jamet, and M. van Schilfgaarde, *Computer Physics Communications* **249**, 107065 (2019).
 - [7] Calculations are done in the full-potential linearized muffin-tin orbital method.[6] Convergence parameters were chosen as follows: basis set *spdf* – *spd* spherical wave envelope functions plus augmented plane waves with a cut-off of 3 Ry, augmentation cutoff $l_{max} = 4$, **k**-point mesh, $12 \times 12 \times 2$. The monolayer slabs were separated by a vacuum region of 3 nm.
 - [8] T. J. Atherton, C. A. M. Butler, M. C. Taylor, I. R. Hooper, A. P. Hibbins, J. R. Sambles, and H. Mathur, *Phys. Rev. B* **93**, 125106 (2016).
 - [9] Supplemental material contains information on the DFT results for various Li locations on the surface unit cell, the band structures for Na and Be covered CoO_2 monolayers, and partial occupation with Li on both surfaces. It also contains details on the entanglement spectrum results and the numerical charge evaluation in the tight-binding model.
 - [10] D. Obana, F. Liu, and K. Wakabayashi, *Phys. Rev. B* **100**, 075437 (2019).
 - [11] S. S. Pershoguba and V. M. Yakovenko, *Phys. Rev. B* **86**, 075304 (2012).
 - [12] R. S. K. Mong and V. Shivamoggi, *Phys. Rev. B* **83**, 125109 (2011).
 - [13] L. Fidkowski, *Phys. Rev. Lett.* **104**, 130502 (2010).
 - [14] A. M. Turner, Y. Zhang, and A. Vishwanath, *Phys. Rev. B* **82**, 241102 (2010).
 - [15] P. Calabrese, *Journal of Physics A: Mathematical and Theoretical* **49**, 421001 (2016).
 - [16] A. Alexandradinata, T. L. Hughes, and B. A. Bernevig, *Phys. Rev. B* **84**, 195103 (2011).
 - [17] H.-B. Yang, Z. Wang, and H. Ding, *Journal of Physics: Condensed Matter* **19**, 355004 (2007).
 - [18] H.-B. Yang, Z.-H. Pan, A. K. P. Sekharan, T. Sato, S. Souma, T. Takahashi, R. Jin, B. C. Sales, D. Mandrus, A. V. Fedorov, Z. Wang, and H. Ding, *Phys. Rev. Lett.* **95**, 146401 (2005).
 - [19] D. Qian, L. Wray, D. Hsieh, L. Viciu, R. J. Cava, J. L. Luo, D. Wu, N. L. Wang, and M. Z. Hasan, *Phys. Rev. Lett.* **97**, 186405 (2006).
 - [20] T. Shimojima, K. Ishizaka, S. Tsuda, T. Kiss, T. Yokoya, A. Chainani, S. Shin, P. Badica, K. Yamada, and K. Togano, *Phys. Rev. Lett.* **97**, 267003 (2006).
 - [21] L. Hong, L. Hu, J. W. Freeland, J. Cabana, S. Ögüt, and R. F. Klie, *The Journal of Physical Chemistry C*

SUPPLEMENTAL MATERIAL

Density functional theory results.

In this section of the supplemental material, we provide additional information on various density functional theory results.

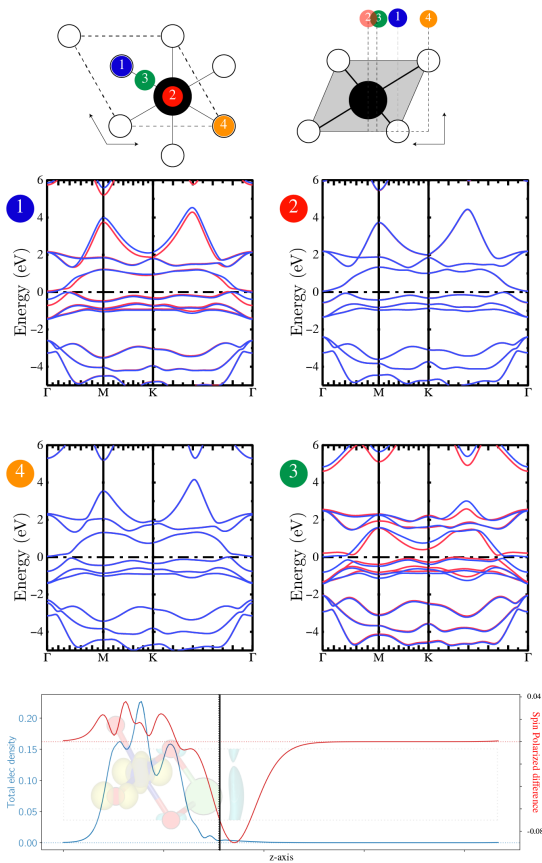


FIG. 4. (*top*) top and side view of all 4 symmetric positions of Li on top of 2D CoO₂ lattice. (*middle*) Spin polarized LDA band structures for the corresponding structures. (*bottom*) Total electron density (blue) integrated along in-plane axis and spin difference $=n_{\downarrow} - n_{\uparrow}$ (red). Black line shows the real space limit for integrating the surface charge density

In Fig. 4 we show the changes in band structure for different surface locations of the Li. Their relative total energies are given in Table I. The lowest energy position (1) for Li is on top of the Co, position (2) is above the bottom O, (4) above the top layer O and (3) in the center of the 2D cell.

It is interesting to note that in structure (3) shown in Figure 4, the effective interaction is between Li and CoO₂ layer is mediated by O-*p* instead of Co-*d*. This change is captured in the band structure by the lowering

TABLE I. Relative energy of the structures in Figure 4

Structure	1	2	3	4
Energy (eV/f.u.)	0	0.09	0.32	0.81

of the center of the *free-electron* like Li band compared to other cases. On the other hand, this is clearly not the lowest total energy. Interestingly, we find negligible spin-polarization for both locations (2) and (4).

At the bottom of Fig. 4 we show the 2D planar averaged electron density and its spin polarization for location (1) set against the structure. The region over which we integrated the surface density is to the right of the vertical black line.

Next we show the band structures for various other cases in Fig. 5. Part (a) shows the case of a monolayer of CoO₂ compensated by one Li per Co but with Li arranged at half the surface density on each surface. The Li atoms then occur in rows. The corresponding electron density is shown in Fig. 6. While showing some electron density just above the Li atom rows, it should be pointed out that this electron density is a factor 10 times smaller than for the full Li coverage. Correspondingly, we see that the surface bands related to Li do not dip below the Fermi level. Although centered at about the same energy, the band width of this surface band is now about 3 times smaller because the Li only have 2 neighbors (along the 1D rows) instead of 6 in the plane. This prevents this surface band to become occupied. However, from the color coding (red for the Li contribution to the band) we can see that the highest occupied band does contain some Li contribution and forms an electron pocket around Γ . The plot of the corresponding wave function modulo squared is what is shown in Fig. 6. This Li row related 1DEG cannot be explained within the SSH4 based tight-binding model. It would require a more complete description of the Li-CoO₂ layer interactions.

Next, in Fig. 5(b) we show the case of a fully Na covered CoO₂ monolayer with Co on one side. This is similar to the corresponding Li case discussed in the main part of the paper but show that with Na, the electron pocket around Γ is increased in size. This is consistent with the larger lateral interactions between Na. Finally, in Fig. 5(c) we show the case of Be covered CoO₂. Compared to Li, we now overcompensate the CoO₂. In this case the electron density in the surface 2DEG is even larger but we also obtain a larger spin-splitting.

Tight-binding model surface charge calculation

In Fig. 7 we show the results of a numerical calculation of the surface state occupancy as function of the energy separation of the two surface bands within the tight-binding approximation. We can see that it is in

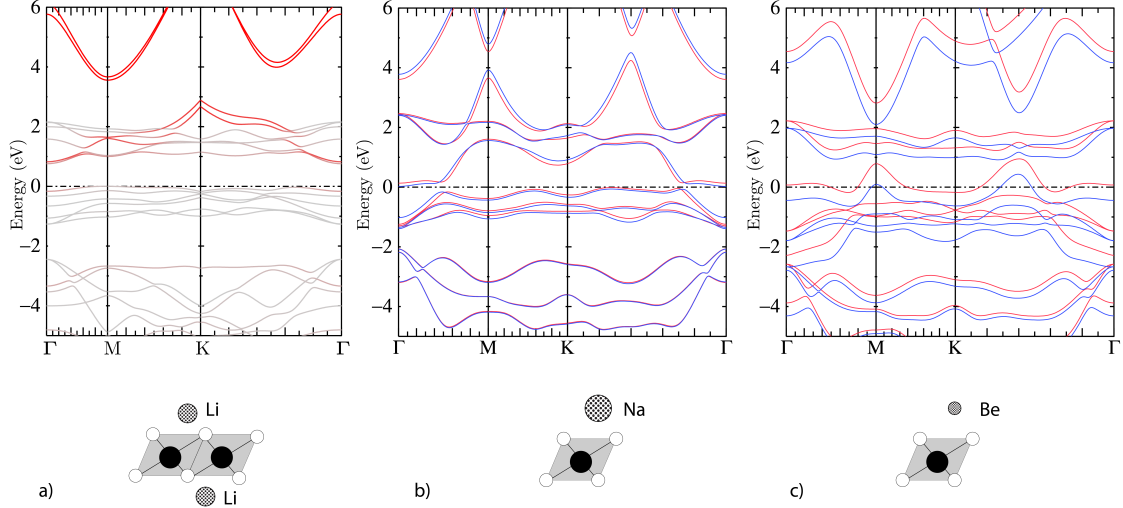


FIG. 5. (a) LiCoO₂ mono-layer with the Li atoms forming 1D chain (Red color is the Li projected band); (b) NaCoO₂; (c) BeCoO₂ band structures (red/blue bands denote the majority and minority spins).

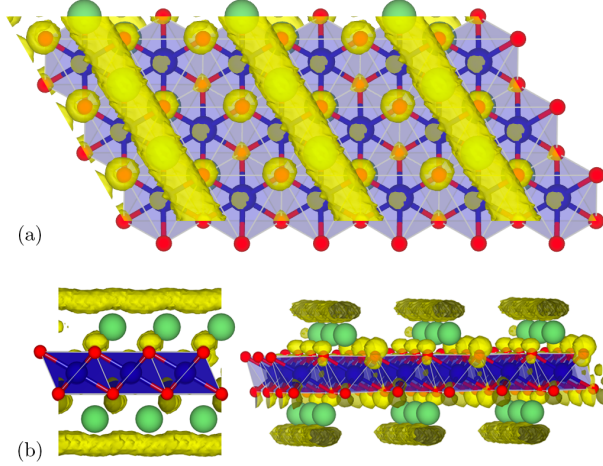


FIG. 6. 2D electron density in case of CoO₂ monolayer with Li on either side but arranged in rows of Li, achieving one Li per CoO₂. yellow isosurface of the electron density correspond to 1.04×10^{-5} .

good agreement with the model results in the main paper. Note that beyond $\delta = 3$ here the overlap of the bands is zero and no charge occurs on the Li side. For $\delta = 0$ we are in the limit where the charge on the Li is 1/2 by symmetry.

Entanglement spectrum

To understand the surface states better, we use the idea of *entanglement spectrum* (ES)[?] which has been found to be a generally useful theoretical tool in inves-

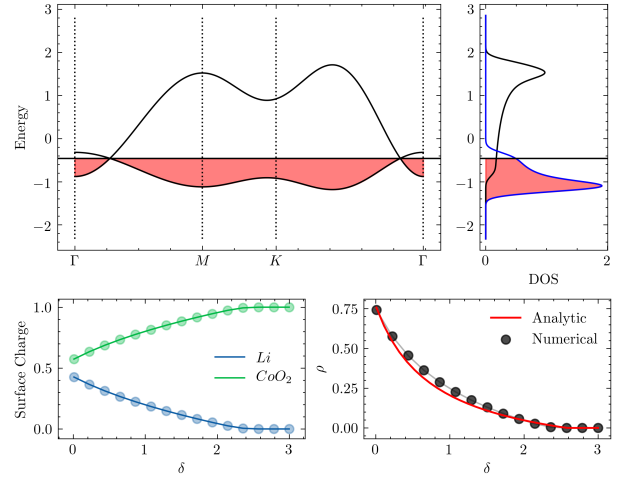


FIG. 7. (Top) Low energy band structure of surface states and Density of States (DOS) contribution from each band (black on Li side, and blue on CoO₂ side) Surface states have a 2D dispersion corresponding to a triangular lattice with nearest neighbor hopping parameters given by $t_{CoO_2}^{xy} = 0.1$ and $t_{Li}^{xy} = -0.3$ in arbitrary units with an on-site offset of $\delta = 0.9$ (in units of $\Gamma/6 = (t_{CoO_2}^{xy} + t_{Li}^{xy})$), (Bottom left) Surface charge per unit cell area as function of on-site parameter δ ; (Bottom right) Ratio of charge on Li to charge on CoO₂ surface layers from numerical TB and analytic equation Eq.(6) derived in the main text. In the limit of $\delta = 0$, this ratio approaches 1.

tigations of topological states[13–16]. The main idea of the ES is that the eigenvalues of the hermitian correlation matrix of the occupied eigenstates, restricted to a subsystem A of the combined system (A+B), provide already information on the existence of surface states when the system would be split in separate A and B

parts and of the topologically non-trivial nature of the system. In our case of non-interacting electrons, the correlation matrix is defined in terms of the Bloch functions expanded in the tight-binding basis set as follows. Although our system is periodic in x and y direction we here consider Bloch states only in one direction combined with the layer direction z in which the non-trivial SSH4 topology applies. Let the eigenstates be $|\psi_{k_x}^n\rangle = e^{ik_x x} |u_{nk_x}\rangle = \sum_{j\alpha} e^{ik_x x} [u_{k_x}^n]_{j\alpha} |\phi_{j\alpha}\rangle$, where i labels the sites, which can be either in the A or B part of the system and α labels orbitals per site, then the correlation matrix restricted to the A-subsystems is given by

$$C_{i\alpha,j\beta}^A(k_x) = \sum_n^{occ} [u_{k_x}^n]_{i\alpha}^* [u_{k_x}^n]_{j\beta}, \quad \text{with } i \in A, j \in A \quad (7)$$

If we remove the restrictions on i, j then we drop the superscript A . The eigenvalues of this correlation matrix $\xi(k_x)$ define the ES. If we would not include the restriction, this correlation matrix is built from idempotent projection operators and thus has eigenvalues 0 or 1 only. As shown in [16] and elsewhere, the existence of eigenvalues deviating strongly from 0 or 1, near 1/2 are an indicator of the entanglement of the states between its subparts and thus of the non-trivial topology and the existence of surface states.

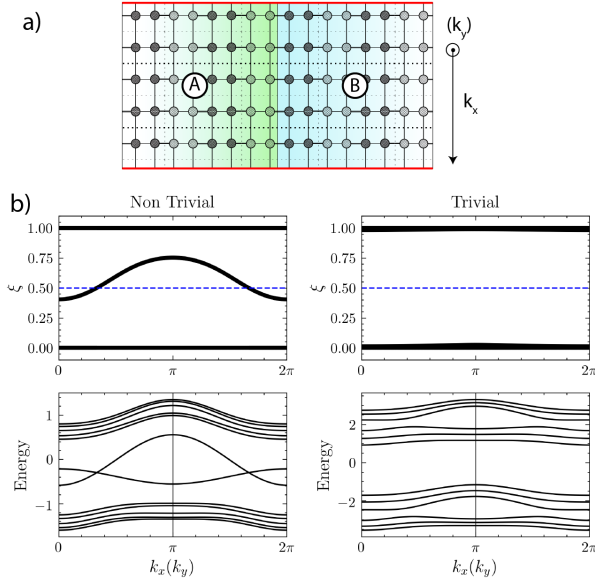


FIG. 8. a) Partitioning of the system in two parts for calculating the entanglement spectrum of the reduced 2D system b) (top) entanglement spectrum of the 2D system along the cut (bottom) band structure of 1D ribbon of the corresponding 2D Hamiltonian showing the edge states for the (left) topologically non-trivial and right trivial choice of SSH4 parameters.

The eigenvalues $\xi(k_x)$ of $C_{ij}(k_x)$ matrix at a given k_x are shown in Figure 8(b) along with the 1D eigenvalues of

our tight-binding model and clearly show the one-to-one correspondence between the ES containing eigenvalues near 1/2 with the existence of surface states. Furthermore we see that for a different choice of the SSH4 TB parameters, no surface states exist and correspondingly no ES with eigenvalues near 1/2.

The connection between ξ and the previous topological picture in terms of cylinders in Fig. 3 of the main paper, is that for each \mathbf{k}_{\parallel} the eigenvalues $\xi > 0.5$ ($\xi < 0.5$) correspond to a loop above (below) the $z = 0$ plane in Fig. 3 of the main paper as indicated by the green/red color in the cylinders of Fig. 3(a). The $\xi = 0.5$ eigenvalue corresponds exactly to the $z = 0$ plane.

-
- [1] K. Mizushima, P. Jones, P. Wiseman, and J. Goode-nough, Materials Research Bulletin **15**, 783 (1980).
 - [2] K. Miyoshi, K. Manami, R. Sasai, S. Nishigori, and J. Takeuchi, Phys. Rev. B **98**, 195106 (2018).
 - [3] K. Iwaya, T. Ogawa, T. Minato, K. Miyoshi, J. Takeuchi, A. Kuwabara, H. Moriwake, Y. Kim, and T. Hitosugi, Phys. Rev. Lett. **111**, 126104 (2013).
 - [4] K. G. Pachuta, E. B. Pentzer, and A. Sehirlioglu, Journal of the American Ceramic Society **0** (2019), 10.1111/jace.16382.
 - [5] Y. Masuda, Y. Hamada, W. S. Seo, and K. Koumoto, Journal of Nanoscience and Nanotechnology **6**, 1632 (2006).
 - [6] D. Pashov, S. Acharya, W. R. Lambrecht, J. Jackson, K. D. Belashchenko, A. Chantis, F. Jamet, and M. van Schilfgaarde, Computer Physics Communications **249**, 107065 (2019).
 - [7] Calculations are done in the full-potential linearized muffin-tin orbital method.[6] Convergence parameters were chosen as follows: basis set *spdf* – *spd* spherical wave envelope functions plus augmented plane waves with a cut-off of 3 Ry, augmentation cutoff $l_{max} = 4$, \mathbf{k} -point mesh, $12 \times 12 \times 2$. The monolayer slabs were separated by a vacuum region of 3 nm.
 - [8] T. J. Atherton, C. A. M. Butler, M. C. Taylor, I. R. Hooper, A. P. Hibbins, J. R. Sambles, and H. Mathur, Phys. Rev. B **93**, 125106 (2016).
 - [9] Supplemental material contains information on the DFT results for various Li locations on the surface unit cell, the band structures for Na and Be covered CoO_2 monolayers, and partial occupation with Li on both surfaces. It also contains details on the entanglement spectrum results and the numerical charge evaluation in the tight-binding model.
 - [10] D. Obana, F. Liu, and K. Wakabayashi, Phys. Rev. B **100**, 075437 (2019).
 - [11] S. S. Pershoguba and V. M. Yakovenko, Phys. Rev. B **86**, 075304 (2012).
 - [12] R. S. K. Mong and V. Shivamoggi, Phys. Rev. B **83**, 125109 (2011).
 - [13] L. Fidkowski, Phys. Rev. Lett. **104**, 130502 (2010).
 - [14] A. M. Turner, Y. Zhang, and A. Vishwanath, Phys. Rev. B **82**, 241102 (2010).
 - [15] P. Calabrese, Journal of Physics A: Mathematical and Theoretical **49**, 421001 (2016).

- [16] A. Alexandradinata, T. L. Hughes, and B. A. Bernevig, Phys. Rev. B **84**, 195103 (2011).
- [17] H.-B. Yang, Z. Wang, and H. Ding, Journal of Physics: Condensed Matter **19**, 355004 (2007).
- [18] H.-B. Yang, Z.-H. Pan, A. K. P. Sekharan, T. Sato, S. Souma, T. Takahashi, R. Jin, B. C. Sales, D. Mandrus, A. V. Fedorov, Z. Wang, and H. Ding, Phys. Rev. Lett. **95**, 146401 (2005).
- [19] D. Qian, L. Wray, D. Hsieh, L. Viciu, R. J. Cava, J. L. Luo, D. Wu, N. L. Wang, and M. Z. Hasan, Phys. Rev. Lett. **97**, 186405 (2006).
- [20] T. Shimojima, K. Ishizaka, S. Tsuda, T. Kiss, T. Yokoya, A. Chainani, S. Shin, P. Badica, K. Yamada, and K. Togano, Phys. Rev. Lett. **97**, 267003 (2006).
- [21] L. Hong, L. Hu, J. W. Freeland, J. Cabana, S. Ögüt, and R. F. Klie, The Journal of Physical Chemistry C **123**, 8851 (2019).